Thesis Preparation Project

Dorothy Xiaoyu Wang szn992
Supervised by Kim Lefmann

Block1, Fall 2022

Contents

1 Introduction

Pyrolytic graphite is often used in neutron instruments, for instance in monochromators and analyzers, which use Bragg scattering. Phonon scatterings happen in pyrolytic graphite and these would cause background. Therefore, the part of the instruments that contain pyrolytic graphite is often cooled to reduce the phonons. Lots of pyrolytic graphite is used in the BIFROST instrument at ESS, and there are some considerations on if the instrument should be cooled. For this reason, the effects of pyrolytic graphite have been carefully studied by experiments and modeling of the experimental data by the simulation package McStas. However, McStas could not simulate phonons in pyrolytic graphite correctly due to the current phonon component.

Therefore, in this project, I worked on improving the phonon component in McStas by applying Born-von Karman phonon scattering. In the new version, both longitudinal and transverse forces are taken into consideration. At the same time up to fourth-nearest neighbors are considered. With this improvement, a better model of pyrolytic graphite would be achieved. By the end of the project, I built a McStas simulation based on the real experiment setup, from the paper *Lattive Dynamics of Pyrolytic Graphite*[1], and simulated the experiment using the new component to check that the new pyrolytic graphite phonon component worked as we expected.

2 Methods

2.1 McStas

McStas is a neutron ray-tracing scattering package, which uses the Monte Carlo method. It simulates a large number of neutrons that have some initial energy according to the manually set distribution. Different components can be placed in the simulated system to simulate the effect of, for instance, a monochromator, a velocity selector, and a collimator... Some neutrons would be lost before hitting the sample if they do not satisfy the criteria of the components that they are passing through. As the neutrons hit the sample, it would lose or gain energy depending on the target. Some detectors in the end would capture the neutrons, when they exit the simulated system and yield results, for example, the energy distribution of the exiting neutrons. In a real experiment, these pieces of information can be used to reveal the characteristics of the sample.

2.2 Born-von Karman Theory

This section is extracted and paraphrased from section 2 of *Modeling realistic scattering from Born-von Karman phonons in copper and pyrolytic graphite with McStas* [4]. Born-von Karman Theory describes an atomic lattice vibration model. The theory assumes that the force on an atom linearly depends on its displacement from its equilibrium position, $u_i(t)$, and its distance to the

neighboring atoms,$u_j(t)$. By combining this expression of force with Newton's second law, for i^{th} atom

$$M_i \frac{d^2 u_i(t)}{dt^2} = \sum_j F_{i,j}^{\alpha}(t), \tag{1}$$

where M_i is the mass of the i^{th} atom, and $\sum_j F_{i,j}^{\alpha}(t)$ stands for the total force on the atom. It can be assumed that the motion of the atom is in the form of a harmonic plane wave. In the specific case when phonon is considered, Equation 1 becomes

$$\omega_{q',p}^2 e_{q',p} = \frac{1}{M} \mathcal{D}(q') e_{q',p}, \tag{2}$$

where ω, e stands for is vibration frequency, polarization direction, and $\mathcal{D}$ is Fourier transformed force constant. In my project, the eigensystem in Equation 2 is solved, and the vibration frequency can be solved.

3 McStas Simulation

Before working on the McStas simulation, I first modified the function omega_q phonon in the component for pyrolytic graphic based on the MATLAB file [2] Kim Lefmann wrote based on Born-von Karman theory and force constants for graphite from the reference paper[1]. The new omega_q function is used to calculate energy transmission, by using force constants from the paper [1], the location of each atom relative to the origin atom, to construct form force constant matrices, with up to fourth-nearest neighbors, and solving for the eigensystem to get the energy for each of the modes of phonon in pyrolytic graphite.

In a triple-axis spectrometer, like in Figure 1, the neutrons are scattered three times before the detector: the first time is at the monochromator, where the energy of the incoming beam (E_i) is selected by scattered an angle $2\theta_M$; the second time is at the sample, by scattered an angle $2\theta_S$; and the third time is at the analyzer, like a monochromator, by scattered an angle $2\theta_A$.

My McStas simulation of triple-axis neutron spectrometer, following the actual experiment[1], was made with components of a Source_Maxwell_3, a monochromator (with Be crystal), a collimator (with divergence 40'), a Phonon_BvK_PG (the new pyrolytic phonon component), another monochromator (used as analyzing crystal) and a PSD_monitor (for detecting scattered neutrons).

3.1 Calculations of Angles in the Scattering Triangle

Four angles need to be specified in the simulation are $2\theta_M$, $2\theta_S$ (2θ), $2\theta_A$ and $A3$, and $A3$ is the rotation of the sample.

First, I focused on the two angles, $2\theta_S$ and α, that are around the sample, where $2\theta_S$ is the angle between $\vec{k_i}$ and $\vec{k_f}$ and α is the angle between $\vec{k_i}$ and $\vec{q}$.

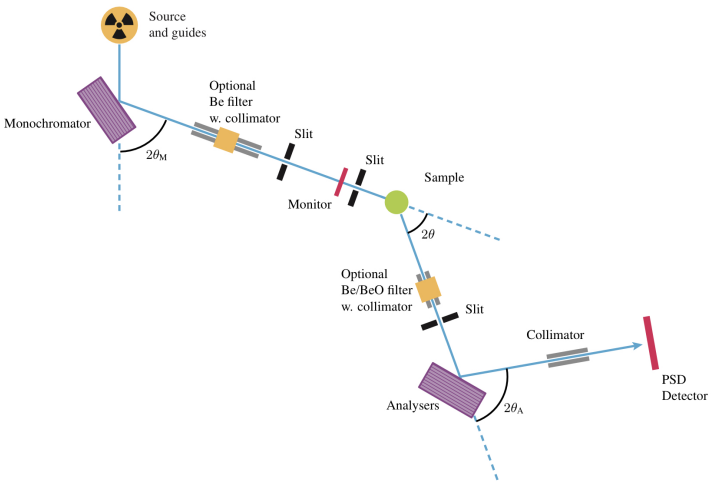

Figure 1: A sketch of a triple-axis spectrometer[3]

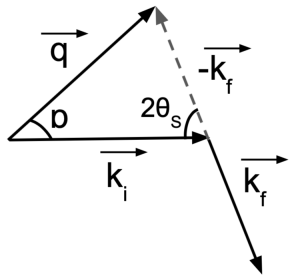

Figure 2: Scattering triangle around the sample

$2\theta_S$ could be calculated directly from the scattering triangle as demonstrated in Figure 2, and $A3$ could be derived from α in the scattering triangle. With known E_i and E_f, all other parameters can be calculated. I calculated the magnitude of wave vectors $\vec{k_i}$ and $\vec{k_f}$ with

$$|k| = (\frac{2Em_n}{\hbar^2})^{\frac{1}{2}}. \tag{3}$$

Since

$$\vec{q} = \vec{k_i} - \vec{k_f}, \tag{4}$$

I rearranged the equation, squared both sides, and got

$$|\vec{q}|^2 = |\vec{k_i}|^2 + |\vec{k_f}|^2 - 2|k_i||k_f|cos(2\theta_S), \tag{5}$$

and

$$|\vec{k_f}|^2 = |\vec{k_i}|^2 + |\vec{q}|^2 - 2|k_i||q|cos(A3), \tag{6}$$

Then I rearranged it again and arrived at

$$2\theta_S = arccos(\frac{|\vec{q}|^2 - |\vec{k_i}|^2 - |\vec{k_f}|^2}{-2|k_i||k_f|}), \tag{7}$$

$$\alpha = arccos(\frac{|\vec{k_f}|^2 - |\vec{k_i}|^2 - |\vec{q}|^2}{-2|k_i||q|}). \tag{8}$$

Since I only aimed to check the dispersion relation along [100] direction and along [001] direction, my simulation only took directions $[h0l]$ into consideration. For hexagonal lattice $[h0l]$ follows

$$\vec{q} = h\vec{a^*} + l\vec{c^*}. \tag{9}$$

$\vec{a^*}$ and $\vec{c^*}$ are in reciprocal space and

$$|a^*| = \frac{4\pi}{\sqrt{3}}\frac{1}{a}, \tag{10}$$

$$|c^*| = \frac{2\pi}{c}. \tag{11}$$

From the referencing paper[1],

$$a = 2.45\mathring{A}, \tag{12}$$

$$c = 6.70\mathring{A}, \tag{13}$$

so

$$|q| = \sqrt{h^2|\vec{a^*}|^2 + l^2|\vec{c^*}|^2}. \tag{14}$$

Note that I have calculated α, which is the angle of $\vec{q}$ relative to $\vec{k_i}$. However, I still needed to calculate the angle of rotation of the sample based on this angle α, h, and l, so that the rotation of the sample could result in the designated direction of the sample facing the incident beam.

From Equation 9 and Figure 3, by some trigonometry, I arrived at the expression:

$$lc^* = |q|sin(A3 + \alpha), \tag{15}$$

and

$$ha^* = |q|cos(A3 + \alpha), \tag{16}$$

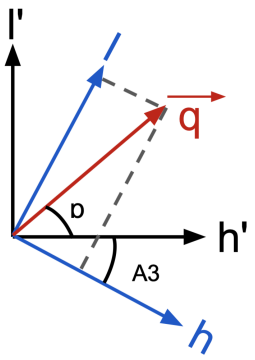

Figure 3: A sketch of the relation between $A3$, α, h and l

where $A3 + \alpha$ is the rotation angle of $\vec{q}$ in hl lattice frame. $A3$ could be solved from Equation 14 and Equation 15 or Equation 16. Since the cosine function is even, the sign of the angle is unknown, therefore, it would be easier to use Equation 15. Then I arrived at

$$A3 = arcsin(\frac{lc^*}{|q|}) - \alpha. \tag{17}$$

When I ran the simulation, I noticed a problem, $\vec{q}$ did not point in the direction I set it in. Therefore, I tried to rotate $A3$ with an additional $\pm 90°$, to check if h and l had been flipped. When $A3$ was rotated with an extra $-90°$, $\vec{q}$ was finally pointed in the direction I set.

In my simulation, following the reference paper[1], the frequency of the reflected beam should be fixed at $6THz$, which indicates that

$$E_f = h\nu \approx 4.136eVHz^{-1} \cdot 6THz \approx 24.8meV. \tag{18}$$

Two other angles, that needed to be determined, are $2\theta_M$ and $2\theta_A$. I used Bragg's Law to calculate them with E_i and E_f. From Bragg's Law

$$\frac{|q_{mono}|\lambda}{4\pi} = sin\theta, \tag{19}$$

I rearranged it:

$$\theta = arcsin(\frac{|q_{mono}|\lambda}{4\pi}), \tag{20}$$

while

$$\lambda = \frac{2\pi}{k}. \tag{21}$$

For the convenience, I also calculated the parameter cluster $\frac{m_n}{\hbar^2}$ in advance:

$$\frac{m_n}{\hbar^2} \approx \frac{1.675 \cdot 10^{-27} kg}{(6.582 \cdot 10^{-16} eV \cdot s)^2} \tag{22}$$

$$\approx 1.506 \cdot 10^{41} m^{-4} kg^{-1} s^2 \tag{23}$$

$$\approx 0.241 \mathring{A}^{-2} meV^{-1}. \tag{24}$$

3.2 Running Simulations

The first step was to find a Bragg point, where the energy absorption or emission is zero.

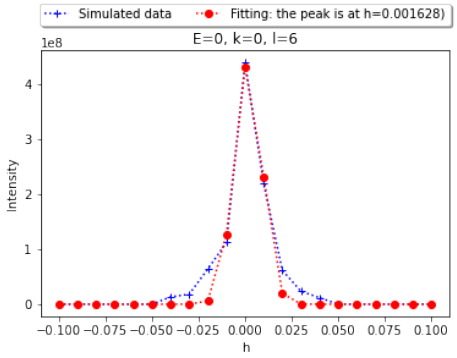

Figure 4: Bragg point at 006

As Figure 4 shows, 006 is a Bragg point. Then, from this point, to find the dispersion relation along [100], I fixed h and scanned through a range of energy transfer E to find the Bragg peak. Then I used Python to fit the peak with a Gaussian distribution and found the energy transfer at that h at the peak. From this process, I obtained one point on the dispersion relation plot. Then I repeated the same procedure and fixed h at different values and repeated the whole process to all the modes. Finally, I plotted all the data points mode by mode. Similarly, when finding the dispersion relation along [001], instead of fixing h, I fixed l at each point. I will compare my simulated result with the experimental data from the paper [1] in the next section.

4 Results and Discussion

4.1 Results Overview

I plotted all the simulated results along with the experimental data Kim Lefmann extracted [2] from the paper [1] in Figure 5 for dispersion relation along [100], and in Figure 6 for that of along [001]. It can be seen from the plots that, for most of the modes, my simulated data lies close to the experimental data

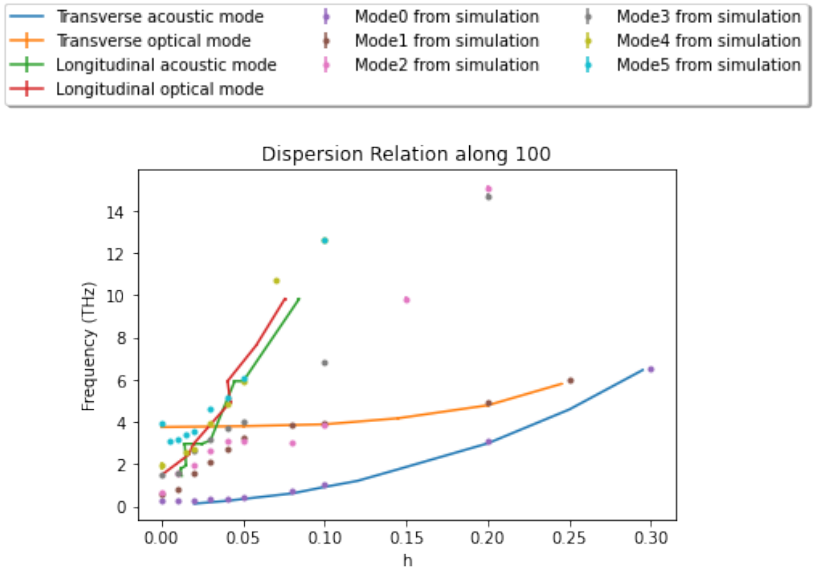

Figure 5: Compare dispersion relation along 100 from simulation to experimental data from the paper[1]

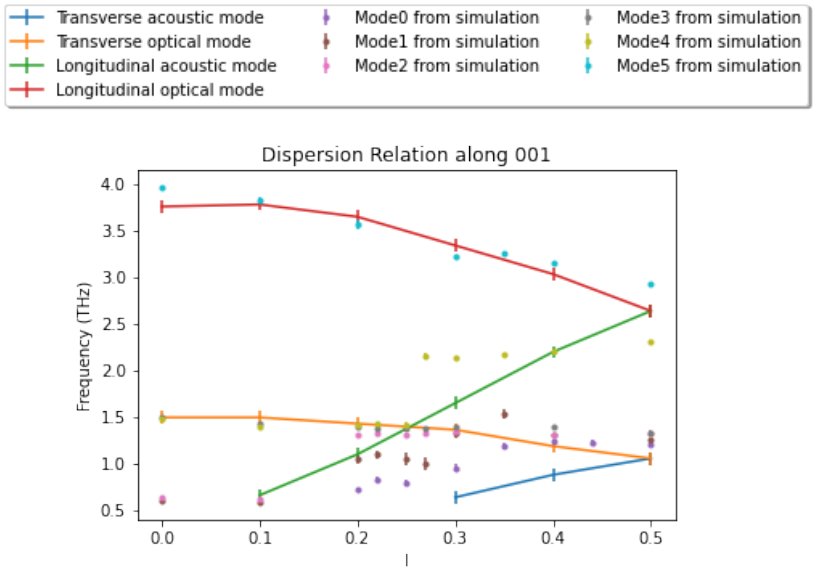

Figure 6: Compare dispersion relation along 001 from simulation to experimental data from the paper[1]

from the paper. However, for instance, the simulated data for mode 2 and mode 3 in Figure 5 is not close to any of the modes observed in the experiment. These could be the transverse modes that could not be measured in a real experiment. Simulated mode 1 and mode 4 in Figure 6 at l greater than around 0.25, also do not match the experimental data that well. I also observed something unexpected as I was fitting the raw data from the simulation, and I will go through them one by one in Section 4.2.

4.2 Problems from the Simulation

4.2.1 Multiple Peaks Observed at Some h or l

I noticed that some of my raw data have multiple peaks, and some of the second-largest peaks have an amplitude almost as big as the peak with the largest amplitude from the same set of data.

I sort the "extra" peaks into three categories: small (S) (see example in Figure 7), medium (M) (see example in Figure 8), and large (L) (see example in Figure 9).

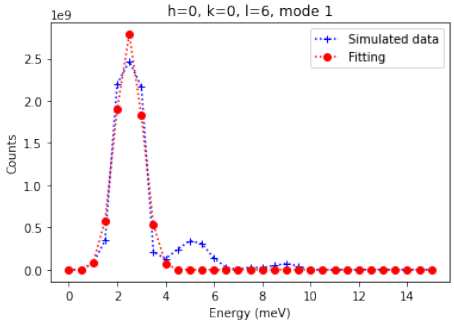

Figure 7: An example of a small "extra" peak

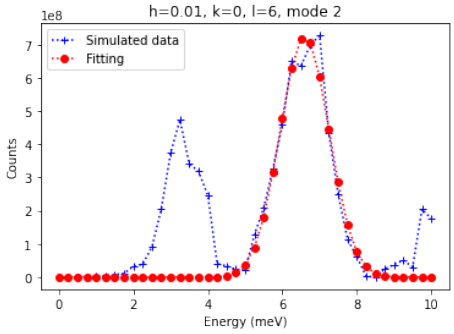

Figure 8: An example of a medium "extra" peak

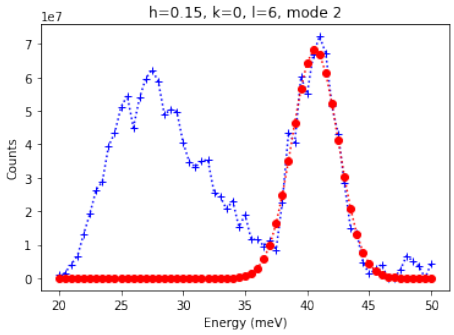

Figure 9: An example of a large "extra" peak

The "extra" peaks I observed in raw data along [100] are located at the following h values:

- Mode1: 0 (S), 0.01 (S), 0.02 (M);
- Mode2: 0 (S), 0.01 (M), 0.15 (L);
- Mode3: 0 (S), 0.02 (M);
- Mode4: 0 (S), 0.02 (M);
- Mode5: 0.005 (S), 0.01(S), 0.015 (M), 0.02 (M).

The majority of raw data for [001] directions has a small "extra" peak. I observe a medium or a large "extra" peak at the following l values:

- Mode1: 0.2 (M), 0.22 (M), 0.25 (L), 0.27 (L), 0.35 (M);
- Mode3: 0.5 (M);
- Mode4: 0 (M), 0.25 (L), 0.27 (M).

4.2.2 Peaks with Long Tails and Large Width at Relative Higher Energy

At energy higher than approximately $40meV$, a large tail is observed, and the peak has a width, much larger than that of at a smaller energy. See an example in Figure 10. This could be due to some resolution issue.

4.2.3 Different Peaks Observed when Measuring the Dispersion Relation Relative to 002

It could be a good idea to simulate the dispersion relation with cold neutrons, to reach a higher resolution. I will show the reasoning through an error propagation below.

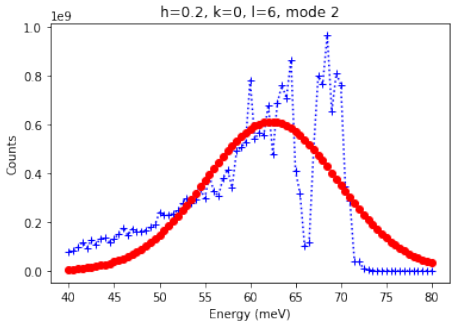

Figure 10: An example of a peak with a large tail and large width

The angle is scattering at the monochromator follows the Bragg Law:

$$n\lambda = 2dsin\theta, \tag{25}$$

where n is the diffraction order; λ is the wavelength; d is the distance between the planes; *theta* is the angle between the deflected beam and the surface. Among these parameters, I simply set $n = 0$, so that here only the first-order diffraction is considered. d is also quite accurate, so the uncertainty of λ mainly comes from the uncertainty of θ. Therefore,

$$\delta\lambda = 2dcos\theta\delta\theta. \tag{26}$$

Meanwhile, Equation 3 can be rearranged to an expression of E and find δE as a function of $\delta\lambda$:

$$E = \frac{\hbar^2 k^2}{2m_n} \tag{27}$$

$$= \frac{\hbar^2 (2\pi)^2}{2m_n \lambda^2}, \tag{28}$$

and

$$\delta E = -\frac{\hbar^2 (2\pi)^2}{m_n \lambda^3}\delta\lambda. \tag{29}$$

Then, plug Equation 26 and Equation 25, into Equation refeq:dE, and get

$$\delta E = -\frac{\hbar^2 (2\pi)^2}{m_n \lambda^3} 2dcos\theta\delta\theta \tag{30}$$

$$= -\frac{\hbar^2 2dcos\theta}{m_n 2\pi}\frac{(2\pi)^3}{\lambda^3}\delta\theta \tag{31}$$

$$= -\frac{\hbar^2 2dcos\theta}{m_n 2\pi}k^3\delta\theta \tag{32}$$

$$\propto E^{3/2}. \tag{33}$$

From Equation 30, it can be seen that the uncertainty of the energy is positively correlated to $E^{3/2}$. Therefore, the cold neutrons, which have smaller energy, could lead to smaller uncertainty of energy, and thus better resolution.

To simulate the cold neutrons, I set $E_f = 10$, and took some data centered around 002. I tried to take a few data points. However, for instance, when I set $h = 0$, $k = 0$, and $l = 2$ and scan through some transfer energy E, I noticed that the peak was at a different location than when I simulated around 006. This difference can be seen in Figure 12. I expected that the peaks should locate at the same energy, and should be at $0meV$. From my raw data, at $0meV$, the counts for both sets of data are non-zero.

Note, when the data is taken at a $\vec{k}$, it takes the number of states within a shell about that $\vec{k}$, like in Figure 11. For a phonon, the density of states can be

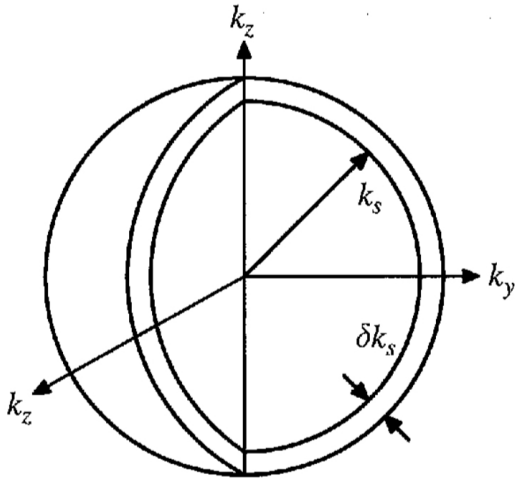

Figure 11: A thin shell of states of wave vector between k_s and $k_s + \delta k_s$[5]

expressed as

$$D(\omega) = \frac{dN}{d\omega} = (\frac{VK^2}{2\pi^2})(\frac{dK}{d\omega})[6], \tag{34}$$

where N is the number of states; ω is the angular frequency; V is the volume; and K is the wave vector. From Equation 34 and Equation 3, the density of states follows a concave up parabola, which means at larger energy, or K, more states are there. When the resolution is not that great, a thicker shell is considered. Therefore, the peaks go up after $0meV$, and I expect that the energy of the peak and the width would vary correlating to the resolution.

I will show my brief investigation in section 4.2.4. The cold neutron, which corresponds to the peak at 002, has a peak at around $0.43meV$, which is closer to $0meV$, than the peak at 006, which is at around $1.00meV$.

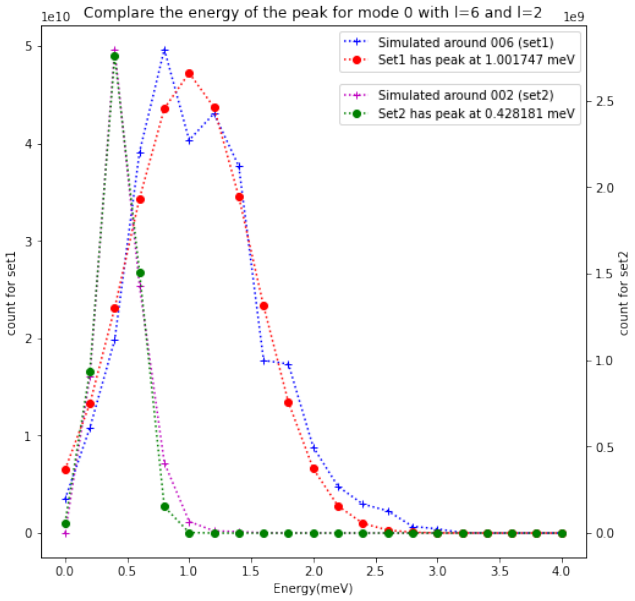

Figure 12: Compare the energy of the peaks centered around 006 and 002 with the same h and k values

4.2.4 Test with Higher Resolution

One thing that is worth trying is to increase the resolution by adding more collimators and see if there are any changes. I added a few collimators so that there is one before and after the monochromator and the analyzer while decreasing the y-height and focus_yh of the sample.

To see if increasing resolution helps with some of the problems I addressed, I first redo the scan as in Figure 10 in Section 4.2.2. Figure 13 shows that with higher resolution, the peak has a slightly smaller width.

I also redo the scan as in Section 4.2.3, and got Figure 14 and Figure 15. It can be seen that the peaks did move slightly closer to zero.

4.3 Suggestions for the Future

After adding the collimators, more neutrons were lost on the way. I only did a quick test on these issues with limited statistics in Section 4.2.4. It would be a good idea to investigate these problems more systematically in the future, for example, to run the whole simulation again, with better resolution, and to see if the simulated data aligns better with the experimental data better.

Meanwhile, as I have addressed in Section 3.1, in the component file, h and l are swapped in the current version. It would be good to have this problem fixed, as well.

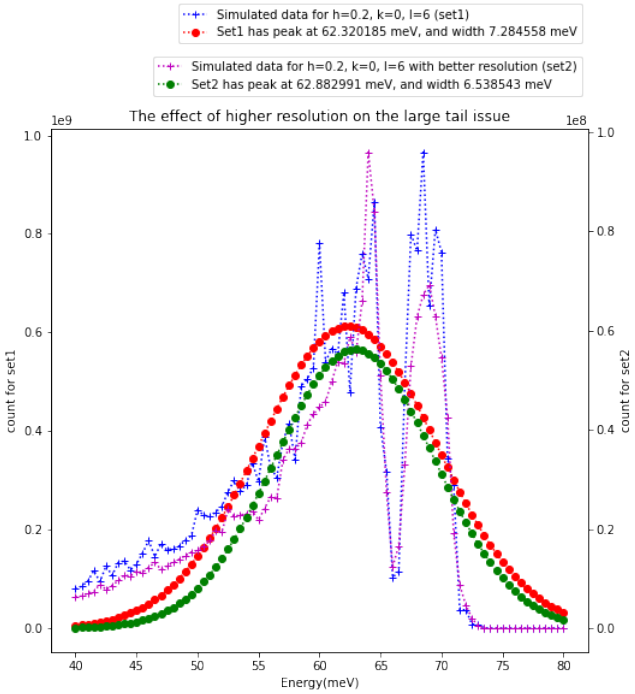

Figure 13: The effect of higher resolution on the large tail problem

References

[1] Nicklow, R., et al. "Lattice Dynamics of Pyrolytic Graphite." Physical Review B, vol. 5, no. 12, 1972, pp. 4951–4962., `https://doi.org/10.1103/physrevb.5.4951`.

[2] Kim Lefmann "BvK_phonon_PG.m"

[3] Kim Lefmann "Neutron Scattering Theory, Instrumentation, and Simulation", University of Copenhagen, 2022.

[4] Kristine M. L. Krighaar, et al. "Modeling realistic scattering from Born-von Karman phonons in copper and pyrolytic graphite with McStas." in preparation

[5] Annett, James F. "1.2 Bose-Einstein statistics." Superconductivity, Superfluids, and Condensates, Oxford University Press, Oxford, 2013.

[6] Kittel, Charles. "5 Phonons II. Thermal Properties." Introduction to Solid State Physics, Wiley, Hoboken, NJ.

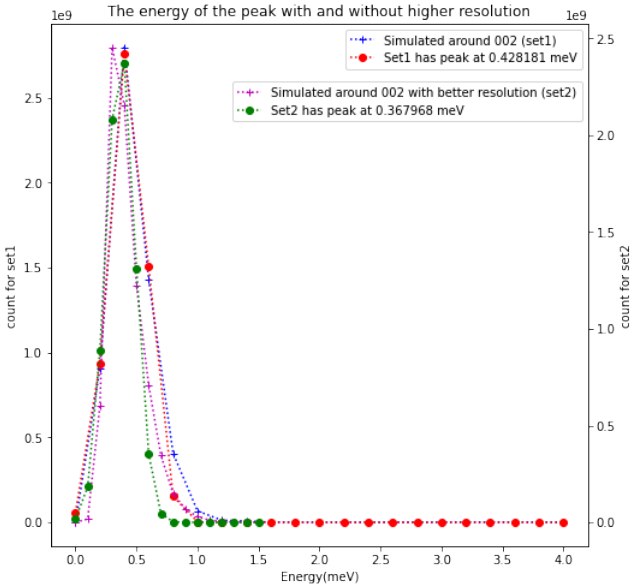

Figure 14: Bragg peak at 002 with and without better resolution

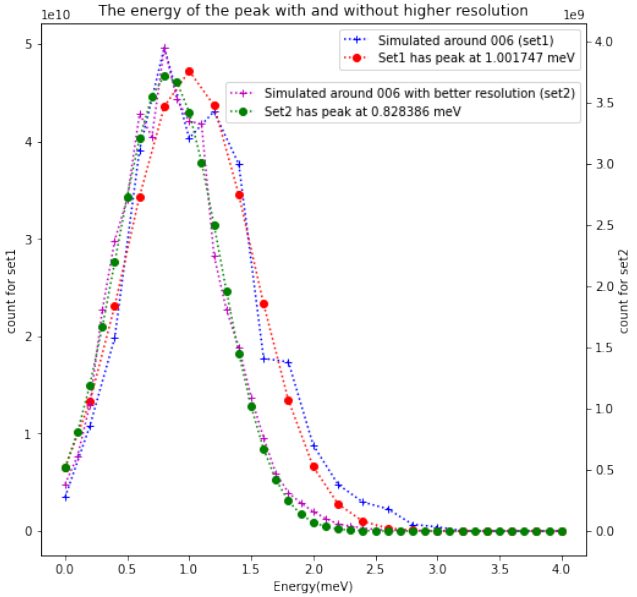

Figure 15: Bragg peak at 006 with and without better resolution